University of Szeged

Faculty of Pharmacy

Institute of Pharmacodynamics and Biopharmacy

Pharmacological and pharmacokinetic characterisation of 2-aminomethylated estrone analogs

Summary of PhD. Thesis

Isaac Kinyua Njangiru

Szeged

2024

University of Szeged, Faculty of Pharmacy

Doctoral School of Pharmaceutical Sciences

Educational program: Pharmacodynamics, Biopharmacy and Clinical Pharmacy

Head of the program: Prof. Dr. István Zupkó, D.Sc.

INSTITUTE OF PHARMACODYNAMICS AND BIOPHARMACY

SUPERVISORS: Dr. Renáta Minorics, PhD.

Prof. Dr. György T. Balogh, D.Sc.

Isaac Kinyua Njangiru

Pharmacological and pharmacokinetic characterisation of 2-aminomethylated estrone analogs

Complex Exam Committee:

Head: Prof. Dr. István Ilisz, D.Sc.

Members: Prof. Dr. István Zupkó, D.Sc.

Dr. Tamás Tábi, Ph.D.

Reviewers Committee:

Head: Prof. Dr. Dezső Csupor, D.Sc.

Reviewers: Dr. Nóra Igaz, Ph.D.

Dr. Mahmoud Al-Khrasani, Ph.D.

Secretary: Dr. Zita Zalán, Ph.D.

Member: Dr. Orsolya Dr. Jójártné Laczkovich, Ph.D.

1. Introduction

Cancer results from genetic and epigenetic factors, causing unique traits in tumor cells as they grow. These traits emerge at different stages due to the gradual accumulation of specific combinations of alterations. In 2019, across 204 countries and territories, there were 23.6 million new cancer cases, resulting in 10.0 million deaths. Moreover, according to GLOBOCAN (Global Cancer Observatory), the global cancer burden is expected to soar to 28.4 million cases by 2040, a 47% rise from 2020.

Cervical cancer ranks fourth globally among women, causing one-fifth of cancer-related deaths**,** especially in low and middle Human Development Index (HDI) countries. In 2018, there were 570,000 cases resulting in approximately 311,000 fatalities. Human Papillomavirus (HPV) infection primarily drives cervical tumor development, alongside genetic and epigenetic changes. High-risk HPV infections, present in 99.7% of cases, lead to dysplastic lesions and cervical cancer, with HPV 16 and 18 being significant subtypes, accounting for about 70% of all cases. Despite the numerous of available treatments, there has been limited progress in disease outcomes over the past two decades. Moreover, relapses, occurring in the range of 10-60%, tend to surface within the initial 2-3 years post-treatment completion. Therefore, the WHO advocates adopting a multifaceted approach to attain these objectives.

Amidst the array of therapeutic approaches, microtubule-targeting agents (MTAs) have emerged as prominent contenders for cancer treatment. By disrupting the normal function of microtubules, MTAs have showcased their effectiveness in impeding cell cycle progression and instigating programmed cell death. Primarily, MTAs disrupt microtubule assembly and spindle formation, culminating in impaired cell division and cell cycle arrest at the G2/M phase, thereby inducing abnormal chromosome segregation. However, notwithstanding their initial efficacy, the emergence of resistance to these agents and the concomitant occurrence of side effects have underscored the necessity for the development of new compounds with reduced resistance and diminished side effects. Thus, researchers have long sought to unravel the intricate biology of cancer, aiming to expedite the development of effective cancer treatments.

Steroids comprise a diverse range of chemical compounds that share a common structural framework: a 17-carbon atom skeleton formed by the fusion of four interconnected rings, consisting of three six-member cyclohexane rings and one five-member cyclopentane ring. They are synthesised from cholesterol, an initial precursor found in steroidogenic organs like the adrenal cortex, placenta, and gonads. Steroids are broadly categorized into sex hormones,

corticosteroids, and neurosteroids. Sex steroids not only exert physiological effects but also play a role in hormone-dependent cancers such as breast, and endometrial cancer.

Research indicates that modifying the structure of 17β-estradiol (E2) can generate estrogen analogs with antiproliferative properties, showing promise as novel anticancer agents, particularly for cervical carcinoma. A-ring-modified 2-methoxyestradiol (2ME), was an early discovery among antiproliferative compounds, with diminished estrogenic properties and showcasing effectiveness against various cancer cell lines. However, limited bioavailability due to poor solubility and rapid hepatic metabolism has been reported, attributed to conjugation and oxidation of hydroxyl groups (-OH) at C-3 and C-17. Researchers aim to leverage 2ME's benefits to create innovative therapeutic analogs with enhanced potency, safety, and improved pharmacokinetics.

The effective design and development of pharmaceutical agents require a deep understanding of physicochemical properties governing drug behaviour in biological systems. Properties such as ionization constant (pK_a), lipophilicity (log$P$/D), topological polar surface area (TPSA), molecular weight (MW), and hydrogen bond donors/acceptors are crucial in determining drug absorption, distribution, metabolism, excretion, and toxicity (ADMET) profiles.

2. Aims of The Study

The objectives of this study were to characterize the physicochemical properties of 2-aminomethylated estrone derivatives and further evaluate their antiproliferative activity against a range of human adherent cancer cell lines. Additionally, the study sought to decipher the anticancer mechanism of action of the most promising compound against the most susceptible cell line.

The specific objectives of the conducted experiments are outlined as follows;

- Characterisation of physicochemical properties particularly; pK_a, log$P$/D$_{7.4}$, TPSA, MW, intestinal permeability and kinetic solubility of 2-aminomethylated estrone derivatives.
- Evaluating the antiproliferative activity of 2-aminomethylated estrone derivatives on selected human adherent gynecological cancer cell lines, and determining their half-maximal inhibitory concentration (IC_{50}) values through MTT assay.
- Assessing tumor selectivity by evaluating the growth inhibition induced by novel compounds on cancer cell lines and comparing it to the effect on a non-cancerous mouse embryonic fibroblast cell line (NIH/3T3).
- Examining the capacity of the selected compound to induce cell morphological changes indicative of apoptosis and necrosis by utilizing Hoechst 33258/propidium iodide fluorescent duo stain (HOPI).
- Investigating the impact of the selected compound on cell cycle progression by flow cytometry.
- Determining the impact of the candidate compound on microtubule dynamics through a cell-independent tubulin polymerisation assay.
- Establishing the antimigratory and antiinvasive effects of the novel compound on cells using wound healing assay and Boyden chamber assay, respectively.
- Assessing the estrogenic-like activity of the test compound via Luciferase assay.

3. Materials and Methods

3.1. Chemical structures of the novel 2ME analogs

A total of 27, 2-aminomethylated estrone derivatives were synthesized at the Department of Molecular and Analytical Chemistry, University of Szeged, Szeged. These derivatives were subsequently classified into three sub-groups (estrone, estradiol, and 17*β*-benzylamino derivatives) and screened for their physicochemical properties and antiproliferative activity. In this study, 2ME was used as a positive control. From the two broader screening criteria of antiproliferative activity and pharmacokinetic properties, the most promising compound, **4a**, was chosen for further analysis. The chemical structure of **4a** is depicted in **Figure 1**.

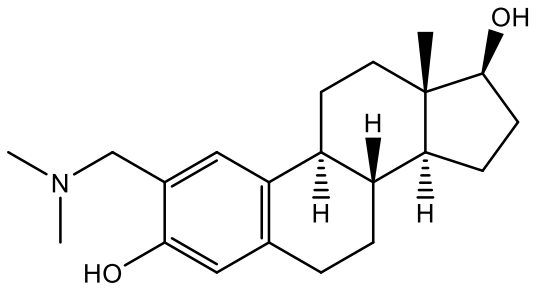

Figure 1. Chemical structure of the tested compound **(4a)**

3.2. Cancer cell lines and culture

The human adherent cervical (HeLa), ovarian (A2780), breast (MDA-MB-231), (MCF7) and (T47D) carcinoma cell lines as well as the non-cancerous mouse fibroblast cells (NIH/3T3), were all obtained from ECACC (European Collection of Authenticated Cell Cultures, Salisbury, UK). The cells were cultured in Eagle's Minimal Essential Medium (EMEM), supplemented with 10% fetal bovine serum (FBS), 1% non-essential amino acid (NEAA) mixture and 1% penicillin, streptomycin, and amphotericin B mixture. Notably, the media used in the maintenance of T47D cells was additionally supplemented with 1% L-glutamine. The culture was maintained at 37°C in a 5% humidified carbon dioxide (CO_2) atmosphere. All media, supplements, chemicals, and kits used in the experiments, unless specified otherwise, were purchased from Capricorn Scientific Ltd. (Ebsdorfergrund, Germany).

3.3. Determination of Antiproliferative Activity by MTT Assay

To assess cell proliferation and viability following treatment with test compounds, a standard MTT (3-(4,5-dimethylthiazol-2-yl)-2,5-diphenyltetrazolium bromide) assay was conducted. Cells were plated onto 96-well microplates at a density of 5000 cells per well. After an

overnight incubation, the cells were exposed to varying concentrations of the test compounds (ranging from 0.1 to 30 μM) and incubated for 24 or 72 hours under standard cell culture conditions. Following the incubation period, MTT solution was added to each well and incubated for 4 hours to allow formazan crystal formation. The formazan crystals were then dissolved by adding dimethyl sulfoxide (DMSO) to the wells. Absorbance values were measured at 545 nm using a microplate reader. Untreated cells served as the control, while 2ME was utilized as a positive control. Dose-response curves were fitted to the obtained data points, and IC_{50} values calculated using GraphPad Prism 5.01 software. Two independent measurements were conducted, each with five replicates.

3.4. *In vitro* physicochemical test methods

Kinetic solubility was tested with 5% (v/v) DMSO as cosolvent in phosphate buffered saline at room temperature for 2 hours using 96-well MultiScreen HTS-PCF Filter Plates (Merck Millipore). Target concentration was 500 μM for the investigated compound. After the incubation period all solutions were filtered by a MultiScreen HTS Vacuum Manifold (Merck Millipore). Concentration of filtrates were determined by spectrophotometric detection ($AUC_{250\text{-}500nm}$) using Multiscan FC Microplate Photometer (Thermo Scientific). The intestinal specific Parallel Artificial Membrane Permeability Assay (PAMPA) investigation was based on a 'in house developed' method. Briefly, a 96-well acceptor plate and a 96-well filter plate were assembled into a sandwich. The hydrophobic filter material of the 96 well filter plate was coated by the mixture of phosphatidylcholine / cholesterol = 2:1 (5 μL, 4 % (w/v) in *n*-dodecane). Subsequently, the acceptor wells at the bottom of the sandwich were dispensed with 300 μL of 10 mM PBS solution adjusted to pH 7.4. The resulting sandwich was then incubated at 37 °C for 4 hours. After the incubation, PAMPA sandwich plates were separated and compound concentrations in donor and acceptor solutions measured, similar to kinetic solubility method. The effective permeability and membrane retention of drugs were calculated as described by Adveef. Additionally, the predicted *in silico* data for the parameters: MW, log*P,* log$D_{7.4}$, p$K_{a,\,acid,}$ most basic character (p$K_{a,\,base}$) TPSA were obtained using a computational software.

3.5. Hoechst 33258–propidium iodide fluorescent double staining

Fluorescence staining was utilized to observe the morphological alterations triggered by apoptosis in cells treated with compound **4a**. HeLa cells were seeded onto 6-well plates at a density of 150,000 cells per well and allowed to incubate for 24 hours before exposure to various concentrations of **4a** (1.0, 2.5, 5.0, and 10 μM) for 48 hours. To differentiate between

apoptotic and necrotic cell populations, cells were stained with lipophilic Hoechst 33258 (1 μg/mL, HO) and hydrophilic propidium iodide (3 μg/mL, PI) for 90 minutes at 37 ˚C in a CO_2 incubator. After removing the residual dye-containing medium, a Nikon Eclipse TS100 fluorescence microscope, equipped with appropriate optical blocks was employed to capture a minimum of 4 images per condition. This methodology enabled the differentiation between early apoptosis and secondary necrosis by evaluating the nuclear morphology and membrane integrity of cells. The HO dye solution easily permeated into the nuclei of all cells, resulting in uniform blue staining in the nuclei of viable cells. The uptake of PI indicated compromised membrane integrity, with cell nuclei exhibiting red staining in cases of late apoptosis or necrosis.

3.6. Cell cycle analysis by flow cytometry

Cell cycle analysis was conducted to elucidate a potential mechanism of action of compound **4a.** Cells were seeded into a 12-well plate at a density of 120,000 cells per well and allowed to incubate overnight. Subsequently, the cells were exposed to 1 ml of freshly prepared EMEM media containing (1.0, 2.5, 5.0, and 10 μM) concentrations of **4a** and incubated for 18, 24 and 48 hours. Supernatants from each treatment were collected separately, and the cells were washed with PBS and detached using trypsin. The resulting cell-containing supernatant was centrifuged at 1300 rpm for 5 minutes, followed by washing with PBS and fixation with 300 μl of 70% ice-cold ethanol at -20°C for 20 minutes. For DNA content staining, cells were treated with 300 μl of staining solution comprising 10 μg/ml PI, 0.1% sodium citrate, 0.1% triton-X, and 10 μg/ml RNase-A, all dissolved in injectable water. The staining process was conducted in the dark for 30 minutes. Cell analysis was performed using a flow cytometer (CytoFLEX-V0-B4-RO, Beckman Coulter), with a minimum of 10,000 events per sample evaluated during each analysis. Data obtained were processed using ModFit LT 3.3.11 software (Verity Software House, Topsham, ME, USA). Untreated cells served as the control group, with apoptotic cells identified as the hypodiploid (subG1) cell population. The cell cycle analysis experiments were conducted twice, with three parallel samples for each condition.

3.7 Tubulin Polymerisation Assay

To determine the effects of test compound **4a** on the microtubular system, a cell-free tubulin polymerisation assay was conducted using a commercially available kit (Cytoskeleton Inc., Denver, Colorado, USA) following the manufacturer's instructions with some adjustments. The assay was carried out in a pre-heated 96-well plate, with each condition tested in two parallel wells. General tubulin buffer served as the experimental control, while 10 μM paclitaxel was designated as the reference compound. Different concentrations of the test compound (50, 150, 300, and 600 μM) were added in equivalent volumes, and the polymerisation reaction was initiated by adding 100 μl of tubulin to each well. Absorbance readings were recorded every minute for 60 minutes at 340 nm, following a kinetic measurement protocol. A parallel experiment was conducted with the exclusion of glycerol from the reaction mixture and involving only 300 and 600 μM concentrations of our test compound. A polymerisation curve was generated from the collected data to illustrate changes in tubulin polymerisation induced by the test compound. The maximum rate of tubulin polymerisation (Vmax) was determined as the greatest difference between the average of a set of three absorbance values at any two consecutive intervals.

3.8 Wound-healing assay

To investigate the antimigratory potential of compound **4a** on HeLa cells, we conducted a wound healing assay using a 2D model, recognizing the significant role of cell motility in tumor metastasis. Special silicon inserts (Ibidi GmbH, Gräfelfing, Germany) were employed, with 50,000 cells per well seeded on 12-well plates in standard EMEM medium, supplemented with 10% FBS. After an overnight incubation, the inserts were gently removed, and the confluent monolayers were washed with PBS. Subsequently, cells were treated with sub-antiproliferative concentrations of **4a** (1.0, 2.5 and 5.0 μM) in EMEM medium containing 2% FBS. Images were captured at 0, 24, and 48-hours post-treatment using a Nikon Eclipse TS100 fluorescence microscope (Nikon Instruments Europe, Amstelveen, The Netherlands). Untreated cells served as the control, and the rate of wound closure (decrease in size of the gaps devoid of cells) was quantified using ImageJ software (National Institutes of Health, Bethesda, MD, USA).

3.9 Boyden chamber assay

The capacity of compound **4a** to inhibit tumor invasion was investigated using the Boyden chamber assay, a three-dimensional model, on a highly invasive HPV-18 positive cell line, HeLa. Prehydrated polyethylene terephthalate (PET) membranes (8 μm pore size) coated with

a thin layer matrigel membrane were inserted into special Boyden chamber inserts (BioCoat™ Matrigel® Invasion Chambers, Corning Inc, Corning, NY, USA) and placed onto a 24 well plate. A cell suspension (50,000 cells/insert in 500 µl) prepared in serum-free EMEM containing sub-antiproliferative concentrations of compound **4a** (1.0, 2.5, and 5.0 µM) was dispensed in the upper compartments. Untreated cells served as controls, with EMEM medium supplemented with 10% FBS acting as a chemoattractant in the lower chambers. After a 24 hour incubation period, supernatants and non-invading cells were carefully removed with a cotton swab. The cells were then washed twice with PBS, fixed with ice-cold 96% ethanol, and stained with 1% crystal violet dye for 30 minutes in the dark. Subsequently, four images per chamber were captured using a Nikon Eclipse TS100 fluorescence microscope (Nikon Instruments Europe, Amstelveen, The Netherlands) and the number of invading cells was quantified using ImageJ software (National Institutes of Health, Bethesda, MD, USA). The invasion rate was determined by comparing the number of invaded cells in the treated samples with the number of invaded cells in the untreated control samples.

3.10 Estrogenic activity assay

The study assessed the estrogenic activity of compound **4a** using T47D-ERE-LucNeo cell line, which expresses estrogen receptor alpha (ERα) and genetically modified to contain a luciferase reporter gene. These cells were cultured in RPMI 1640 phenol red free medium, supplemented with 10% FBS, 1% NEAA, 1% antibiotics and 1% L- glutamine The cells were seeded into microplates, incubated for 72 hours and depleted the intracellular estrogen by changing the medium for several days. On the ninth day, the cells were treated with different concentrations of estrogen E2, 2ME, and the test compound **4a**. After a 24 hour incubation period, luciferase activity was measured using a luminometer. Each concentration was tested in triplicate and repeated twice for reliability. The resulting data were analyzed using GraphPad Prism 9.5.1 software to generate concentration-response curves.

3.11 Statistical analysis

Statistical analysis was performed using GraphPad Prism version 5.01 or version 9.5.1 (GraphPad Software, San Diego, CA, USA). One-way analysis of variance (ANOVA) followed by the Dunnett post-test was used to determine statistical significance. All results shown represent means ± SEM from a minimum of two independent experiments. *, **, and *** denote $P < 0.05$, $P < 0.01$, and $P < 0.001$, respectively, compared to the control.

4. Results

4.1. Antiproliferative Activity and pharmacokinetic properties of compound 4a

Among the compounds under investigation, (2-[(dimethylamino)methyl]-estradiol), designated as compound **4a**, emerged as the most promising candidate based on its tumor selectivity and antiproliferative effect against the HVP-18 positive human cervical cancer cell line (HeLa) (**Table 1**). Furthermore, it demonstrated favourable physicochemical properties compared to the positive control, 2ME (**Table 2**). Consequently, it was chosen for further evaluation to elucidate its mechanism of action.

Table 1. Antiproliferative properties of the newly synthesized compound **4a**

Concentration (µM)		Growth Inhibition; ± SEM [Calculated IC_{50} Value; µM]			
Compound		HeLa	A2780	MB-231	NIH/3T3
4a	10	72.47± 0.76	6.46 ± 2.96		29.15 ± 1.92
	30	90.71± 1.10	64.79 ± 1.56	< 50	38.42 ± 1.64
		[4.53]	[27.53]	n.d	**[70.88]**
2ME	10	92.08 ± 1.24	72.04 ± 2.06	99.25 ±0.52	62.23 ± 0.90
	30	92.59 ± 1.07	80.08 ± 1.81	99.86 ± 0.64	63.63 ± 0.97
		[1.15]	[0.70]	[1.35]	**[2.53]**

2ME: 2-methoxyestradiol; n.d. not determined.

Table 2. *In silico* and experimental physicochemical parameters of compound **4a**

Physicochemical Analysis				In silico data				Lipophilic ligand Efficiency (LLE)			
Compd	Solubility (µM)		GI-PAMPA	MW	TPSA	P*K*a	Log *P*	HeLa	A2780	MB-231	NIH/3T3
	pH 6.5	pH 7.4	$P_e 10^{-6}$ cm/s								
4a	380.3	235.4	11.4	329	43.7	10.2	3.34	**2.00**	1.22		0.81
2ME	52.5	53.9	46.3	302	49.7	10.3	3.36	**2.58**	2.79	2.51	2.24

4.2 Apoptosis inducing effect by fluorescent double staining

After exposing HeLa cells to varying concentrations of compound **4a** for 48 hours, significant changes were observed in cell morphology and membrane integrity. Fluorescence imaging revealed a decrease in viable cell count, correlating with compound **4a**'s concentration. An increase in intense blue fluorescence emanating from the nuclei signified DNA condensation, a characteristic hallmark of early apoptosis. This fluorescence became more pronounced with higher concentrations of the compound. Additionally, red fluorescence suggested the presence of secondary necrotic cells, implying potential damage to cell membranes (**Figure 2**).

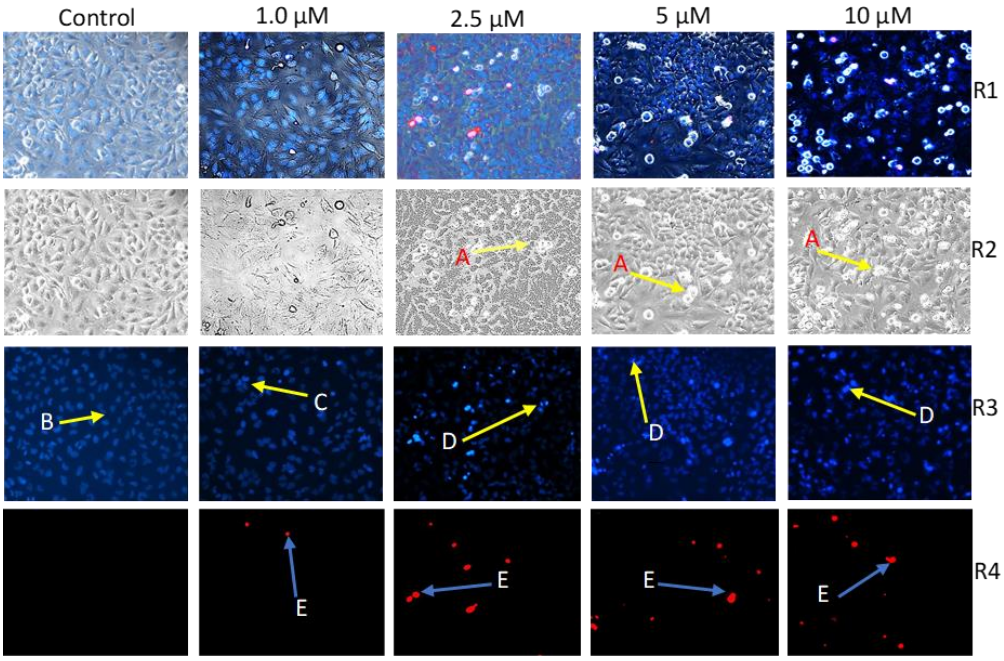

Figure 2. Representative photos of two independent experiments performed on three parallels. Compound **4a** induced morphological changes on HeLa cells (**A**) under brightfield (**R2** panel). Intact (**B**), early apoptotic (**C**), late apoptotic (**D**) and necrotic (**E**) HeLa nuclei stained by Hoechst 33258 (blue fluorescence, **R3** panel) and propidium iodide (red fluorescence, **R4** panel) after 24 h of treatment at four distinct concentrations. The panel **R1**, represents an overlay of corresponding photos from R2, R3 and R4. Photos captured by fluorescent microscopy at 10× magnification.

4.3. Compound 4a induced cell cycle disturbance

The impact of compound **4a** on cell cycle progression was studied *in vitro* over three-time intervals (18, 24 and 48 hours) by analyzing cellular DNA content using PI. Treatment of HeLa cells with compound **4a** resulted in rapid and significant arrest at the G2/M phase, accompanied by a notable increase in the hypodiploid sub-G1 population after 18 hours, across all tested concentrations (1.25, 2.5, 5.0 and 10 µM). Longer incubation periods (24 and 48 hours) led to a concentration-dependent increase only in the sub-G1 population, particularly at higher

concentrations. Statistical analysis focusing on HeLa cells treated with **4a** at 5 µM (corresponding IC_{50} value) revealed significant findings. Notably, there was a significant rise in the sub-G1 phase at 18 and 48 hours compared to 24 hours. Additionally, a significant decrease in the G1 cell population was observed at 18 hours compared to 24 and 48 hours. However, there were no significant differences in the S-phase population across all tested time intervals. Nevertheless, a significant increase in the G2/M population was observed at 18 hours compared to both 24 and 48 hours (**Figure 3**).

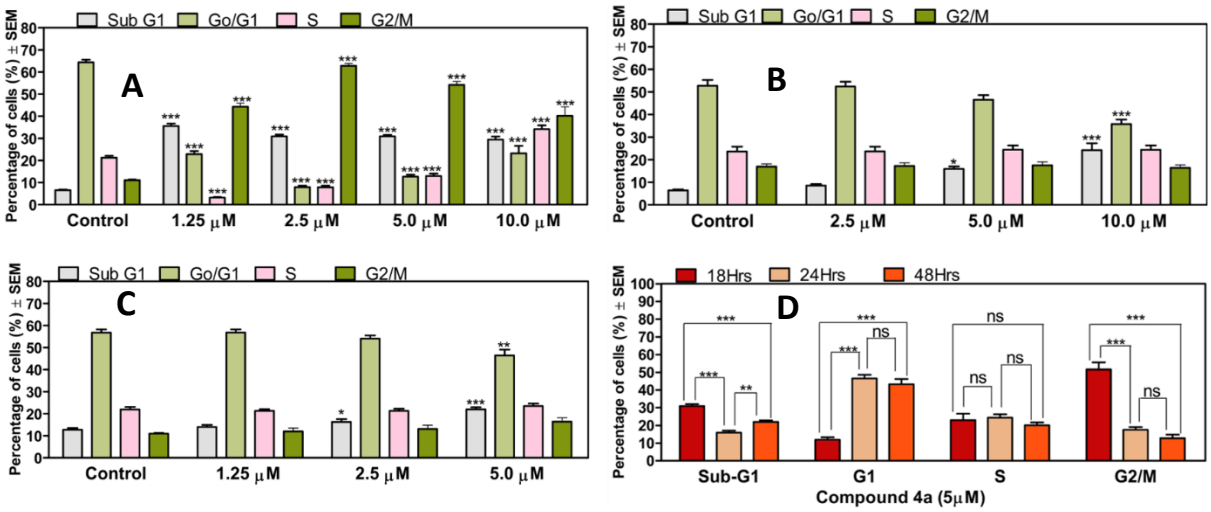

Figure 3. 4a induced cell cycle disturbances marked with significant increase in sub-G1 cell population accompanied with cell blockade at G2/M phase (**A**) observed 18 h post-treatment. Extended incubation for 24 h (**B**) and 48 h (**C**) only resulted in a significant rise in the hypodiploid sub-G1 population at 5, 10 µM and 2.5, 5 µM respectively. Statistical analysis conducted to assess the impact of incubation time on cell cycle progression in HeLa cells treated with **4a** at a concentration of 5 µM (**D**). Results are expressed as mean values ± SEM of the data on three separate measurements with triplicates, *, ** and *** indicate $p < 0.05$, $p < 0.01$ and $p < 0.001$ respectively, compared to untreated control samples.

4.4. Compound 4a lacked swift cytotoxic effects

A study was undertaken to examine cell growth inhibitory effects of **4a** on HeLa cells, with the goal of determining whether **4a** induced rapid cytotoxicity following a 24 hour incubation period. This validation was critical since previous findings on cell cycle progression, conducted after an 18 hours incubation of HeLa cells with **4a**, had shown the induction of apoptosis via a significant increase in the sub-G1 population. The MTT assay results for compound **4a** following a 24 hour incubation period with HeLa cells revealed diminished inhibition in cell growth. Notably, even at concentration corresponding to the IC_{50} of **4a,** there was no significant alteration in cell viability (**Figure 4**).

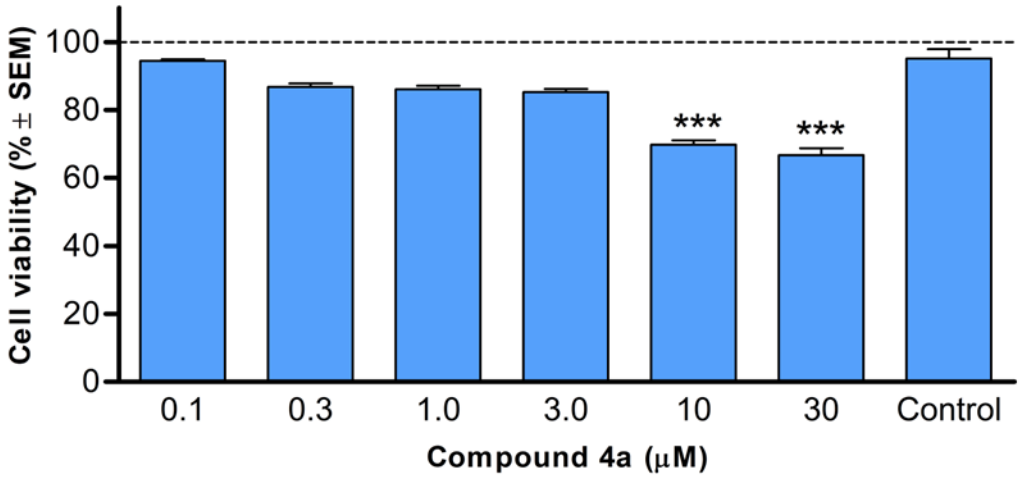

Figure 4. Cell viability of HeLa cells following 24 h incubation with **4a**. Data include two independent experiments conducted with five parallels. Control: untreated cells. Results are expressed as cell viability % ± SEM. *** denote $p < 0.001$. Non-significant changes are not indicated.

4.5. Effects of compound 4a on tubulin polymerisation

To investigate the impact of compound **4a** on microtubule dynamics, a cell-independent tubulin polymerisation assay was conducted in both presence and absence of glycerol. Following the manufacturer's guidelines and taking into account the IC_{50} value of **4a**, concentrations of (50, 150, 300, and 600 μM) of the test compound were examined. In this study, paclitaxel was utilized as a positive control. The results showed that the rate (Vmax) and extent of tubulin polymerisation increased in a concentration-dependent manner, peaking at 300 μM both with and without glycerol (**Figure 5**). Beyond this concentration, there was a notable decrease in the maximum rate of tubulin polymerisation in the presence of glycerol. However, when tested in absence of glycerol, there was no significant difference observed in the maximum rate of tubulin polymerisation between 300 μM and 600 μM concentrations.

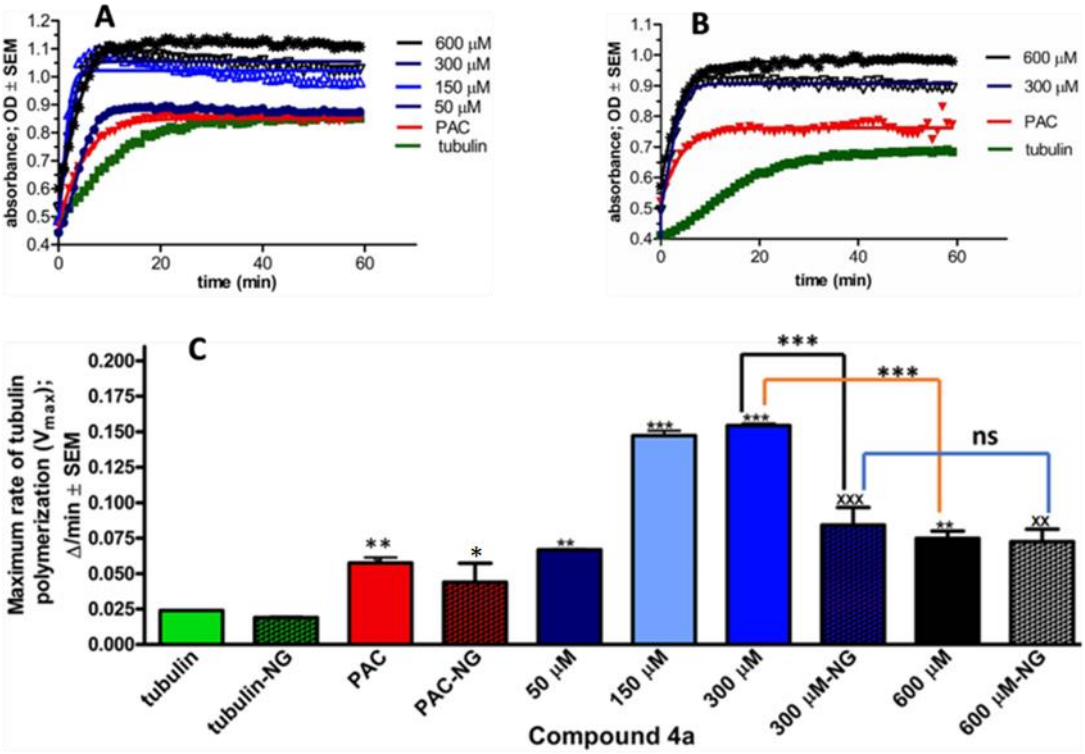

4.6. Antimigratory effects of 4a on HeLa cells

To explore the antimetastatic potential of compound **4a**, necessary to inhibit collective cell movement, a thorough assessment was conducted using a 2D model. This involved evaluating changes in cellular migratory capacity through a wound healing assay, which is crucial in metastasis development. A comparison between treated and untreated controls at 24 hour and 48-hour intervals revealed that compound **4a** exhibits an antimigratory effect, influenced by both concentration and time (**Figure 6**). Image analysis further confirmed a significant reduction in HeLa cell migratory capacity, measuring 53.9% and 39.6% after 24 or 48 hours of treatment with 5.0 µM of the compound, respectively, relative to the control.

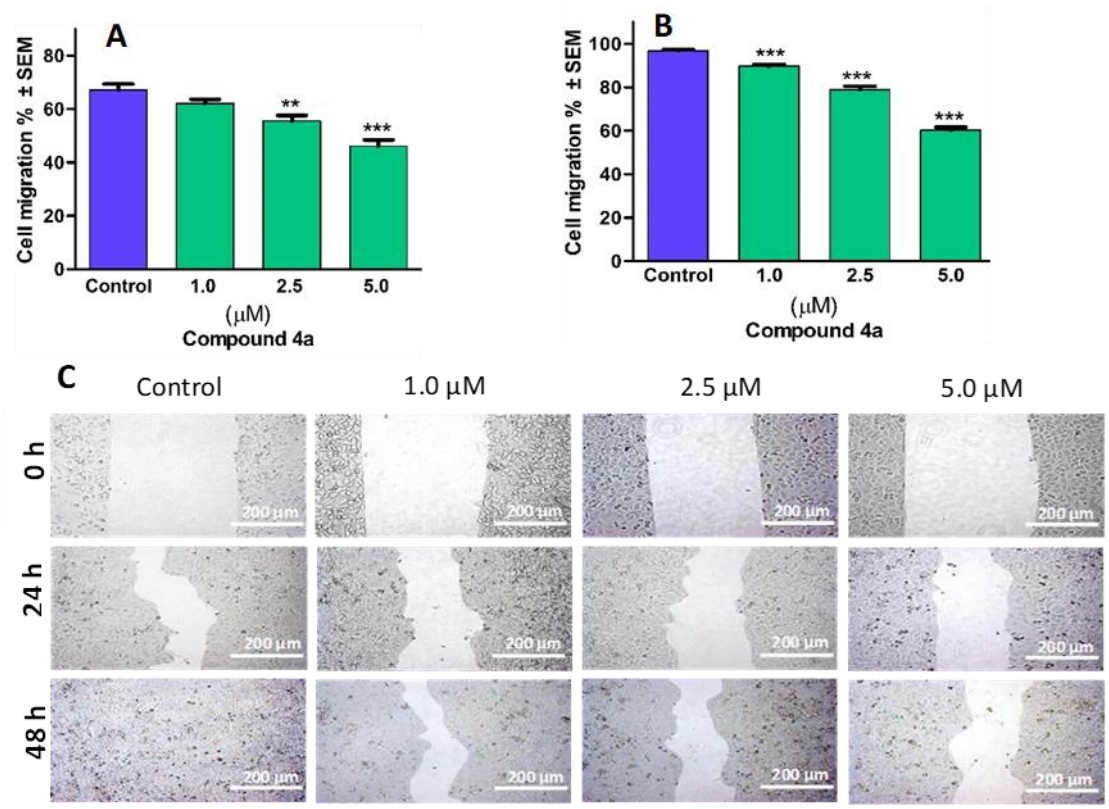

Figure 6. Compound **4a** inhibited migration of cervical cancer cells (HeLa). Quantified rates of wound closure were significantly diminished in the presence of compound **4a.** Graphs indicate the percentage of cell migration at **24 h** (**A**) and **48 h** (**B**) post-treatment of HeLa cells, relative to the control. Representative images of reduced wound healing at **0, 24** and **48 h** post-treatment (**C**). Results are expressed as mean values ± SEM of the data on two separate measurements with triplicates. ** and *** indicate $p<0.01$ and $p<0.001$ respectively, compared to control.

4.6. Tumor antiinvasive activity of 4a on HeLa cells

In evaluating cell invasion in a 3D model using Boyden chamber inserts with a matrigel membrane, we effectively replicated the primary tumor environment by pre-coating the membrane with extracellular matrix proteins. Image-based data collection enabled the calculation of invading cell counts per well, which was then used to determine the percentage of cancer cells that successfully infiltrated the surrounding area. Comparative analysis with control samples revealed a significant and concentration-dependent inhibitory effect of **4a** on cancer cell invasion within the concentration range of 1.0 to 5.0 μM (**Figure 7**). Notably, exposure to a concentration of 5.0 μM for 24 hours resulted in a reduction of more than 95% in the number of invading HPV-18 positive cervical cancer cells.

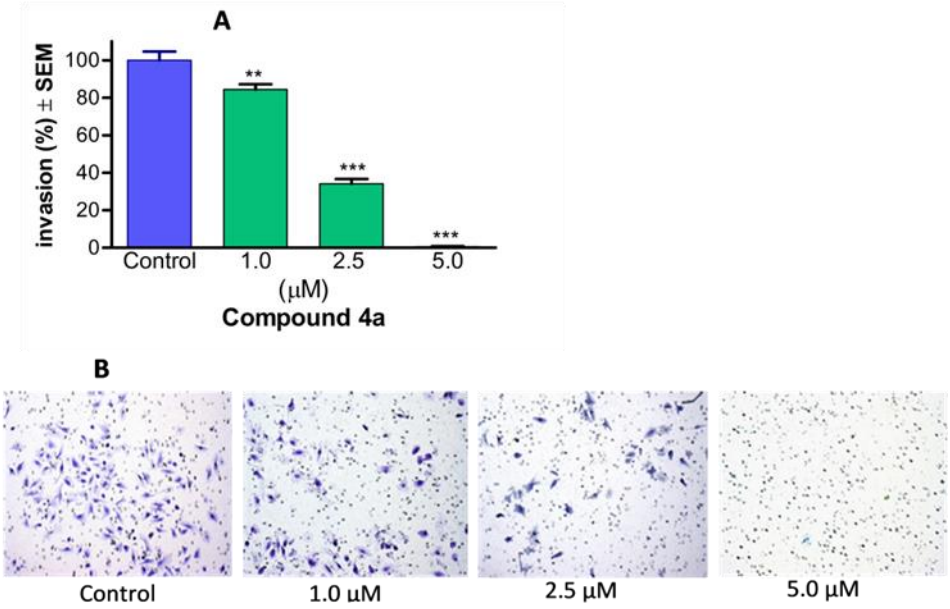

Figure 7. Compound **4a** markedly diminished the invasiveness of cervical cancer cells (HeLa). The anti-invasive potential of the test compound is illustrated by representative images (**B**) and is quantified by the percentage of invading cells in the Boyden chamber containing different concentrations of **4a**, using EMEM medium supplemented with 10% FBS as a chemoattractant (**A**). Results are presented as mean values ± SEM of the data from three separate measurements with duplicates. ** and *** indicate $p < 0.01$ and $p < 0.001$, respectively, compared to untreated control samples.

4.6. Estrogenic activity of compound 4a

Since compound **4a** shares structural similarities with 2ME, both being analogs of E2, their potential estrogenic activities are of interest in understanding their pharmacological characteristics. Our experiment focused on determining the transcriptional activity of the estrogen-dependent luciferase gene transfected into T47D breast cancer cells. Compound **4a** (EC_{50} = 6.53 x 10^{-7} M) and 2ME (EC_{50} = 1.11 x 10^{-8} M) exhibited estrogenic activity at least three orders of magnitude weaker than the positive control, endogenous E2 (EC_{50} = 1.74 x 10^{-11} M) (**Figure 8**). This finding is consistent with previously published data, especially concerning 2ME. Furthermore, compound **4a**, akin to 2ME, displayed antiproliferative, antimetastatic and hormonal activity within the same concentration range.

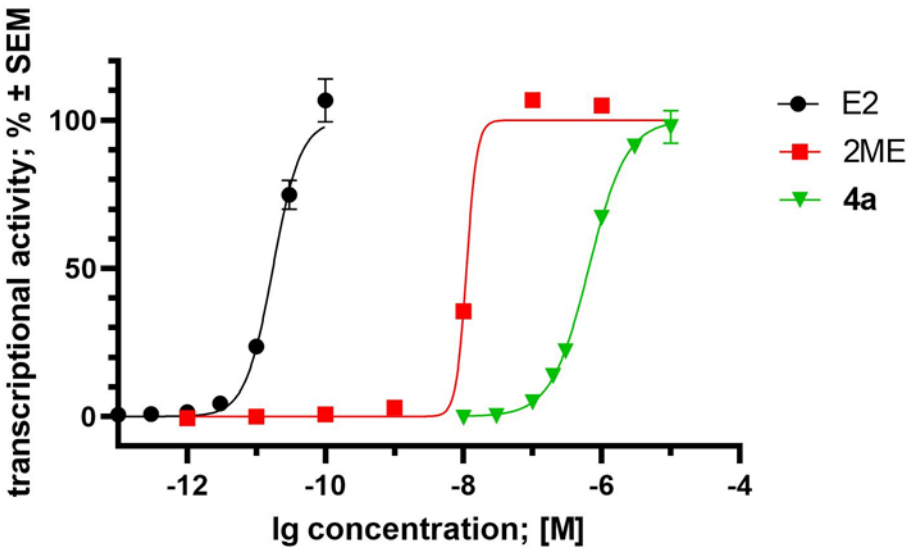

Figure 8. Estrogenic effect of compound **4a**, 2-methoxyestradiol (2ME) and 17*β*-estradiol (E2) expressed as the transcriptional activity of estrogen-responsive luciferase reporter cassette transfected into T47D breast cancer cell line, T47D-ERE-Luc^{Neo}. Data are based on two independent experiments performed in triplicate and are expressed as average ± SEM.

4.7. Antiproliferative Activity of 4a on T47D and MCF7 Breast Cancer Cell Lines

Comparatively, compound **4a** demonstrated a reduced ability to inhibit growth in the ER-α positive breast cancer cell lines T47D and MCF7 when compared to its effect on the cervical cancer cell line, HeLa. Specifically, compound **4a** exhibited an IC_{50} value of 4.53 μM on HeLa cells, whereas on T47D and MCF7 cells, higher IC_{50} values of 16.92 μM and 19.18 μM were observed, respectively.

5. Discussion

Cervical cancer ranks as the fourth most common cancer in women worldwide, accounting for one-fifth of cancer-related deaths. Consequently, there is a pressing need for more effective and better-tolerated drugs to address this particular cancer type.

This study investigated the antiproliferative effects of twenty-seven newly synthesized 2-aminomethylated estrone analogs across diverse human adherent cancer cell lines, encompassing cervical (HeLa), ovarian (A2780), and breast (MDA-MB-231) carcinoma cells. Their selectivity towards tumors was evaluated using a non-cancerous fibroblast (NIH/3T3) cells. Furthermore, their pharmacokinetic properties were also profiled. Among the studied analogs, compound **4a** showcased the most promising drug-like characteristics and was chosen for detailed investigation.

Compound **4a** displayed remarkable antiproliferative activity against the most susceptible cell line (HeLa) and demonstrated the highest tumor selectivity among all the tested compounds. Conversely, 2ME exhibited promising activity against the studied gynecological cancer cell lines, with low IC_{50} values. However, it demonstrated inhibition of non-cancerous fibroblast cells at concentrations below 3 μM, suggesting potential non-selectivity towards tumor cells under the experimental conditions employed.

In terms of the rules of thumb for clinical candidates, notably Lipinski's rule of five (Ro5), the pertinent physicochemical parameters (MW, pKa, $logP/D_{7.4}$, TPSA, kinetic solubility and intestinal-specific PAMPA permeability) of **4a** were generally more favourable than those of 2ME. These attributes supported the choice of **4a** for further investigation aimed at elucidating its possible mechanism of action.

Detailed analysis through HOPI double staining revealed changes in cell morphology indicative of apoptosis, including an increase in cells with condensed DNA post-treatment. Intense blue fluorescence observed in the HO panel further suggests nuclear condensation, a characteristic feature of early-stage programmed cell death. The 48-hour incubation period likely prompted some early-apoptotic cells to progress into late-apoptotic or secondary necrotic stages, as evidenced by the red fluorescence emitted by certain cells stained with PI.

Flow cytometry analysis confirmed the apoptosis-inducing effect of compound **4a** and provided insights into its possible mechanism of action. Treated cells exhibited rapid arrest at the G2/M phase, accompanied by a notable increase in the hypodiploid sub-G1 population after

18 hours of incubation. However, with prolonged incubation for 24 and 48 hours, a significant rise was observed only in the sub-G1 population, with no substantial change in the G2/M population. This increase in the sub-G1 cell population after 18 and 48 hours, along with the rise in the G2/M phase after only 18 hours of treatment with **4a**, may be partially attributed to the activation of the spindle assembly checkpoint (SAC) by as reported with some potent antimitotic agents.

The MTT assay was therefore conducted to evaluate the impact of compound **4a** on the growth of HeLa cells after 24 hours of incubation. The results revealed diminished cell growth inhibition, with no significant change in cell viability at a concentration corresponding to the IC_{50} value of **4a**. Hence, the substantial increase in the sub-G1 population during cell cycle analysis after 18 hours of incubation is likely due to the induction of apoptosis rather than a direct cytotoxic effect of **4a**.

Tubulin polymerization is essential for mitosis, and 2ME inhibits this process by targeting tubulin's colchicine-binding site. We investigated how compound **4a** directly influences tubulin polymerization using a cell-independent system tailored for this purpose. Across all tested concentrations, compound **4a** notably increased tubulin polymerization, albeit showing a decrease in the maximum rate beyond 300 μM. To assess the direct impact of **4a** without glycerol, which promotes tubulin polymerization, we examined its effect in its absence. At approximately 300 μM, **4a** exhibited its maximum effect on tubulin polymerization, with no significant change even at 600 μM. Comparing polymerization rates with and without glycerol indicated similar outcomes at concentrations beyond 300 μM, suggesting full tubulin protein binding even in the presence of glycerol. As there was no substantial difference in **4a**'s effect at 300 μM and 600 μM without glycerol, 300 μM can be considered the optimal concentration for saturating tubulin binding sites with **4a**.

Several studies have highlighted the significant role of metastasis in cancer-related fatalities. Targeting cell migration is crucial for therapeutic intervention to prevent invasion and metastasis, ultimately reducing patient mortality. Certain synthetic compounds, such as 2ME, demonstrate both antimitotic properties and cell antimigratory activity *in vitro*, indicating their potential as anti-cancer agents. In our *in vitro* experimental assay, the drug candidate **4a** demonstrated a remarkable ability to inhibit the migration of highly invasive HeLa cells, in a manner dependent on both time and concentration.

Besides cell migration, tumor metastasis relies heavily on invasion and penetration into surrounding tissues. Thus, we enhanced our cellular migration wound healing assay by including a specialized three-dimensional cell invasion Boyden chamber assay. Our findings showed a concentration-dependent reduction in cell invasion with compound **4a**, reaching over 95% inhibition at 5.0 μM compared to the control. These results align with those reported in a study involving 2ME.

The mechanism of action of 2ME involves binding to the colchicine binding domain on β-tubulin, thereby influencing microtubule dynamics. The results unveiled a high affinity of **4a** for binding to the colchicine binding site, akin to 2ME. Furthermore, computational simulation performed at the Department of Medicinal Chemistry, University of Szeged, identified four residues responsible for the two binding poses. Notably, interaction diagrams of the most robust ligand-protein complexes depicted characteristic hydrogen bonds between the -OH groups of the ligand and specific amino acids, namely ASN101, ASP327, as well as VAL236 and CYS239. Consequently, these findings further corroborate our previous results, indicating the interaction of compound **4a** with tubulin and its subsequent enhancement of tubulin polymerisation.

Compound **4a** was nevertheless, found to exhibits estrogenic activity, as demonstrated in ERα-transfected T47D breast cancer cells. However, it also notably inhibits proliferation and cell motility in HeLa cells, which lack ERα but express ERα-36, a variant form of ERα, lacking the AF-1 region. Despite similarities in ligand-binding domains, **4a**'s interaction differs across signaling pathways. It displays stronger growth inhibition in HeLa cells than in T47D and MCF7 breast cancer cells, which express native ERα. Additionally, besides targeting the colchicine-binding site on tubulin, MTT assay results suggest that **4a**'s impact on the ERα-36 pathway may contribute to the observed effects on HeLa cells. Consequently, further research is needed to fully understand **4a**'s interaction with the cervical ERα-36 receptor.